Renormalization group approach to energy level statistics at the integer quantum Hall transition

Philipp Cain and Rudolf A. Römer*
Institut für Physik, Technische Universität Chemnitz, D-09107 Chemnitz, Germany

Mikhail E. Raikh
Department of Physics, University of Utah, Salt Lake City, Utah 84112

(Dated: *Revision* : 1.22, compiled July 24, 2002)

We apply the real-space renormalization group (RG) approach to study the energy level statistics at the integer quantum Hall (QH) transition. Within the RG approach the macroscopic array of saddle points of the Chalker-Coddington network is replaced by a fragment consisting of only five saddle points. Previously we have demonstrated that the RG approach reproduces the distribution of the *conductance* at the transition, $P(G)$, with very high accuracy. To assess the level statistics we analyze the *phases* of the transmission coefficients of the saddle points. We find that, at the transition, the nearest neighbor energy level spacing distribution (LSD) exhibits well-pronounced level repulsion. We emphasize that a metal-like LSD emerges when the *fixed point* distribution $P_c(G)$ is used. We check that away from the transition the LSD crosses over toward the Poisson distribution. Studying the change of the LSD around the QH transition we observe scaling behavior. Using a finite-size scaling analysis we are able to extract a critical exponent $\nu = 2.37 \pm 0.02$ of the localization length.

PACS numbers: 73.43.-f Quantum Hall effects, 73.43.Nq Quantum phase transitions, 64.60.Ak Renormalization-group, fractal, and percolation studies of phase transitions (see also 61.43.Hv Fractals; macroscopic aggregates)

I. INTRODUCTION

The integer quantum Hall (QH) transition is described well in terms of a delocalization-localization transition of the electron wavefunction. In contrast to an usual metal-insulator transition (MIT), the QH transition is characterized by a single extended state located exactly at the center $\epsilon = 0$ of the Landau band. When approaching $\epsilon = 0$, the localization length ξ of the electron wavefunction diverges according to a power law $\epsilon^{-\nu}$, where ϵ defines the distance to the MIT for a suitable controlled parameter, e.g. the electron energy.

The calculation of the energy level spacing distribution (LSD) is an established method in the study of the properties of an MIT. It relies on the exact knowledge about consecutive eigenenergies of a system. The LSD $P(s)$ then describes the probability to find neighboring energy levels at an energy distance s. At the MIT the wavefunctions of the electrons change from being extended in the metallic to being localized in the insulating regime. This crossover is also observed in the correlation of the corresponding energy levels. Wavefunctions of localized electrons are bound to a small volume in space. Therefore the wavefunctions are spatially uncorrelated which results in an uncorrelated energy spectrum. Thus the LSD is a Poisson distribution. On the metallic side wavefunctions extend over a large part of the sample. The overlap of the wavefunctions creates a correlation in the energy spectrum, which leads to level repulsion for small s. The shape of $P(s)$ in the metallic regime is predicted by random matrix theory (RMT)[1,2] and depends on the universality class the system belongs to. The universality class reflects the symmetry of the Hamiltonian of the system. The following basic Gaussian Ensembles can be distinguished: (i) orthogonal (GOE) with time-reversal invariance and rotational symmetry, (ii) unitary (GUE) with broken time-reversal symmetry but rotational symmetry, and (iii) symplectic (GSE) with time-reversal invariance and broken rotational symmetry. In the case of the QH transition the magnetic field breaks the time-reversal symmetry. It can therefore be classified into the GUE.

Exactly at the MIT a third system-size independent, so called critical LSD $P_c(s)$ is found. The discussion of the shape of $P_c(s)$ concentrates on the behavior in the tails. For small s it is commonly excepted[3–5] that $P_c(s)$ resembles the level repulsion found in the metallic regime. For large s contradicting results have been obtained. Initial numerical studies[6–9] found agreement with the analytic prediction[10] $P_c(s) \propto \exp(-as^\gamma)$ for $s \gg 1$ obtained by mapping the LSD to a Gibbs distribution of a classical one-dimensional gas. The exponent $\gamma = 1 + (\nu d)^{-1}$ is related to the spatial dimension d and the critical exponent of the localization length ν at the MIT. However, later numerical simulations[3,5,11–16] questioned these relations and rather favored a simple exponential decay $P_c(s) \propto \exp(-bs)$ suggested previously by Shklovskii *et al.*[17]. The numerical works capture all mentioned universality classes and are based mainly on tight-binding models, like the Anderson model of localization[18].

From the LSD close to the MIT also the critical exponent of the localization length ν can be computed[19] and its value only depends on the universality class of the problem. Since the exponential divergence of ξ holds only for the infinite system, it is not evaluable directly by numerical methods. Therefore calculations performed for finite system sizes are to be extrapolated by a suitable scaling approach. The resulting ν at the QH transition should agree with the values obtained by various other methods, e.g. $\nu = 2.5 \pm 0.5$[20], 2.4 ± 0.2[21], 2.35 ± 0.03[22], and 2.39 ± 0.01[23].

In order to access the LSD at the QH transition we use the Chalker-Coddington (CC) model[20] which has proven successful in quantitative studies of the QH transition[21,24–34]. The CC model is a strong magnetic field (chiral) limit of a general network model, first introduced by Shapiro[35] and later utilized for the study of localization-delocalization transitions within different universality classes[36–41]. Besides the QH transition, the CC model can be employed to a much broader class of critical phenomena since the correspondence between the CC model and thermodynamic, field-theory and Dirac-fermions models[42–50] has been shown.

In this work we calculate the LSD from the CC model using the real-space renormalization group (RG) approach[23,51–55]. First, in Sec. II we describe the model and how to compute the eigenenergies and the LSD. In Sec. III we present our numerical results for the LSD. The finite-size scaling (FSS) analysis of the obtained LSD at the QH transition is content of Sec. IV. Concluding remarks are presented in Sec. V.

II. MODEL AND RG METHOD FOR LSD

A. Description of the RG approach

The CC model is based on the microscopic picture of electron motion in a strong magnetic field and a smooth disorder potential[20]. This allows to separate the rapid cyclotron motion from the semiclassical trajectories of the guiding center of the cyclotron orbit. Assigning these trajectories to *links* and considering saddle points (SP's) at which different trajectories come closer than the Larmour radius as *nodes* a chiral network can be constructed as shown in Fig. 1. For simplicity, the nodes are placed on a square lattice.

We now apply a real-space RG approach[51,52] to the CC network[56,57]. The RG approach is based on the assumption that a certain part of the network containing several SP's, the RG unit, represents the essential properties of the entire network. This unit is next replaced through the RG transformation by a single *super*-SP with an S matrix determined by the S matrices of the constituting SP's. The network of super-SP's is then treated in the same way as the original network. Successive repetition of the RG transformation yields the information about the S matrix of very large samples, since, after each RG step n, the effective sample size grows by b^n, with b a scale factor determined by the geometry of the original RG unit.[23,58,59] Thus the RG method is very efficient for studying large systems. On the other hand, the RG unit represent only an approximation of the real structure of the underlying network and spatial correlations beyond a distance b are ignored.[23,58,59] The RG unit we use is extracted from a CC network on a regular 2D square lattice as shown in Fig. 1. A super-SP consists of five original SP's by analogy to the RG unit employed for the 2D bond percolation problem[58–60] and $b = 2$. We have shown[23] by comparison with direct numerical simulations that the application of this RG unit yields very accurate results.

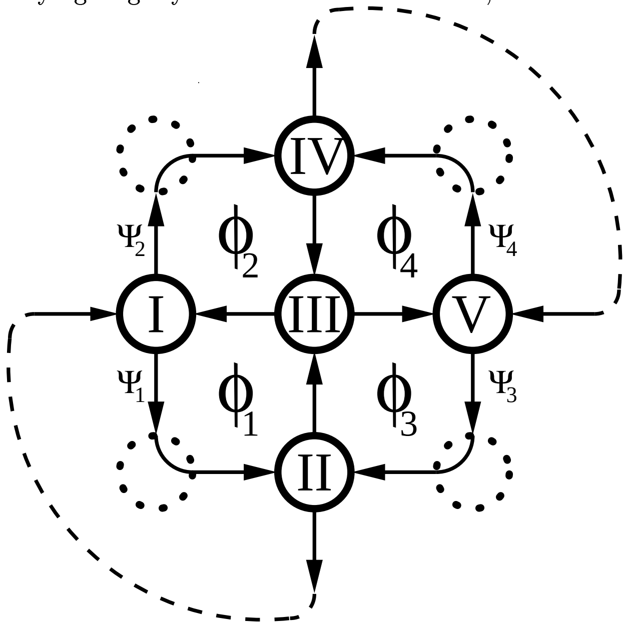

FIG. 1: Network of SP's (circles) and equipotential lines (arrows) on a square lattice. The RG unit used for Eq. (1) combines five SP's (full circles) into a super-SP by neglecting some connectivity (dashed circles). $\Phi_1, \ldots, \Phi_4$ are the phases acquired by an electron drifting along the contours indicated by the arrows. $\Psi_1, \ldots, \Psi_4$ represent wave function amplitudes and the thin, dashed lines denote the periodic boundaries used for the compuation of level spatistics.

Between the SP's an electron travels along equipotential lines, and accumulates a certain Aharonov-Bohm phase. Different phases are uncorrelated, which reflects the randomness of the original potential landscape. Each SP can be described by two equations relating the wave-function amplitudes in incoming and outgoing channels. For our RG unit, this results in a system of ten linear equations, the solution of which yields the following expression for the transmission coefficient of the super-SP (Ref. 52):

$$t' = \left| \frac{t_1 t_5 (r_2 r_3 r_4 e^{\imath\Phi_2} - 1) + t_2 t_4 e^{\imath(\Phi_3+\Phi_4)} (r_1 r_3 r_5 e^{-\imath\Phi_1} - 1) + t_3 (t_2 t_5 e^{\imath\Phi_3} + t_1 t_4 e^{\imath\Phi_4})}{(r_3 - r_2 r_4 e^{\imath\Phi_2})(r_3 - r_1 r_5 e^{\imath\Phi_1}) + (t_3 - t_4 t_5 e^{\imath\Phi_4})(t_3 - t_1 t_2 e^{\imath\Phi_3})} \right| \quad . \tag{1}$$

Here t_i and $r_i = (1-t_i^2)^{1/2}$ are, respectively, the transmission and reflection coefficients of the constituting SP's, Φ_j are the phases accumulated along the closed loops (see Fig. 1). Equation (1) is the RG transformation, which allows one to generate (after averaging over Φ_j) the distribution $P(t')$ of the transmission coefficients of super-SP's using the distribution $P(t)$ of the transmission coefficients of the original SP's. Since the transmission coefficients of the original SP's depend on the electron energy ε, the fact that delocalization occurs at $\varepsilon = 0$ implies that a certain distribution, $P_c(t)$ — with $P_c(t^2)$ being symmetric with respect to $t^2 = \frac{1}{2}$ — is the fixed point (FP) of the RG transformation (1). The distribution $P_c(G)$ of the dimensionless conductance G[23] can be obtained from the relation $G = t^2$, so that $P_c(G) \equiv P_c(t)/2t$.

B. RG approach to the LSD

The LSD describes the probability of next-nearest-neighbor energy level spacings. The evaluation of the LSD therefore relies on the calculation of eigenenergies of the system. Eigenenergies are usually obtained from the time-independent Schrödinger equation $H\Psi = E\Psi$ by diagonalizing the Hamiltonian H[61]. With the CC model based on wave propagation through the sample, H is not accessible directly and a different approach has to be used. It has been shown,[62] that the levels can be computed also from the energy dependent unitary network operator $U(E)$ of the 2D CC network. U is constructed similar to the system of equations for obtaining t' of the RG unit. Its energy dependences stems from the energy dependence of the $t_i(E)$ of the SP's and the $\Phi_j(E)$ of the links of the network. So each SP contributes 2 equations which also contain the phases of the links thus for, e.g., a 50×50 SP network U is a 5000×5000 matrix. When comparing to the calculation of the transmission coefficient t' an essential difference as to be taken into account. Here we are interested in energy levels which are defined only in a closed system. Therefore periodic boundary conditions are applied by connecting the free outgoing with the free incoming links of the RG unit (see Fig. 1: lower to left link, upper to right link). Considering the vector Ψ of wave amplitudes on the links of the network, U acts similar as a time evolution operator. The eigenenergies can now be obtained from the stationary condition

$$U(E)\Psi = \Psi. \tag{2}$$

Nontrivial solutions exist only for discrete energies E_k, which coincide with the eigenenergies of the system[62]. The eigenvectors Ψ_k correspond to the eigenstates on the links. The evaluation of the E_k's according to Eq. (2) is numerically very expensive. For that reason a simplification was proposed.[30] Instead of solving the real eigenvalue problem one calculates a quasispectrum of phases ω following from

$$U(E)\Psi_l = e^{\imath\omega_l(E)}\Psi_l. \tag{3}$$

For fixed energy E the phases ω_l are expected to obey the same statistics as the real eigenenergies. For large networks this approach for computing the LSD was already used previously[30]. We will compare the results of both methods later.

Before we apply a similar approach to the RG of the LSD we have to consider the structure of the RG unit again. It contains 4 closed loops where the electron travels along an equipotential and accumulates a phase. Since the length of the equipotential line obviously depends on the energy of the electron, also the phase is a function of energy. For the functional form of $\Phi_j(E)$ we assume an appropriately chosen simple linear behavior,

$$\Phi_j(E) = \Phi_{0,j} + 2\pi\frac{E}{s_j}, \tag{4}$$

with a random part $\Phi_{0,j}$ uniformly distributed within $[0, 2\pi]$ and a coefficient s_j which defines a periodicity in the sense of $\exp(\imath\Phi) = \exp[\imath(\Phi + 2\pi)]$. In this way s_j acts as a level spacing connected to the loop j of the SP. Its value is chosen from an initial LSD $P(s)$. Later we will study also the influence of other dependencies on E. Note that for simplicity, we shall henceforth assume that the explicit energy dependence of the transmission amplitudes can be ignored.[30]

In order to obtain the E_k's we now have to find solutions of Eq. (3) where $\omega_l(E_k) = 0$ (or $2\pi, 4\pi, \ldots$). In Fig. 2 we show $\omega_l(E)$ for a sample configuration with E_k corresponding to the roots $\omega_l = 0$. By this means the energy dependence of $U(E)$ at the QH transition is governed by the 4 phases, while the 5 SP's are described by the transmission coefficients according to the FP distribution $P_c(t)$. Therefore the set of 10 equations used for the determination of (1) – albeit with periodic boundaries – can now be reduced to 4 equations in which only the phases $\Phi_1, \ldots, \Phi_4$ of the 4 loops are independent. Then we can write Eq. (2) for the 4 wave amplitudes $\Psi_1, \ldots, \Psi_4$ indicated in Fig. 1 as

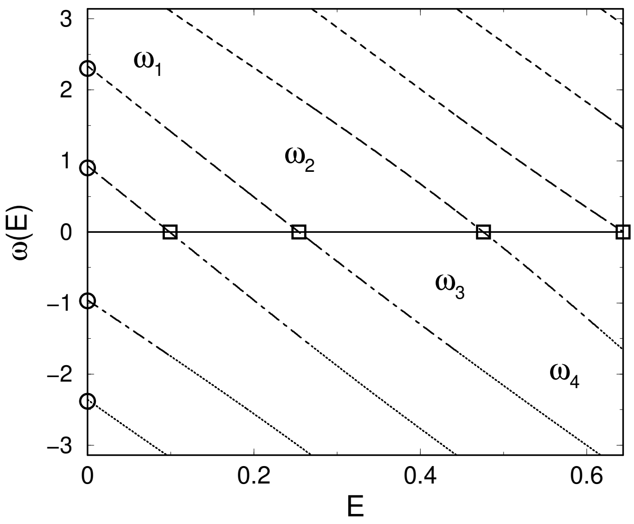

FIG. 2: Energy dependence of the quasieigenenergies ω for a sample configuration. Instead of using the quasispectrum obtained from $\omega_l(E=0)$ ($\bigcirc$) we calculate the real eigenenergies according to $\omega(E_k)=0$ ($\square$). Different line styles distinguish different $\omega_l(E)$ where $\omega_1>\omega_2>\omega_3>\omega_4$.

$$\begin{pmatrix} (r_1r_2-t_1t_2t_3)e^{-\imath\Phi_1} & (t_1r_2+t_2t_3r_1)e^{-\imath\Phi_1} & t_2t_5r_3e^{-\imath\Phi_1} & t_2r_3r_5e^{-\imath\Phi_1} \\ -t_1r_3r_4e^{-\imath\Phi_2} & r_1r_3r_4e^{-\imath\Phi_2} & -(t_4r_5+t_3t_5r_4)e^{-\imath\Phi_2} & (t_4t_5-t_3r_4r_5)e^{-\imath\Phi_2} \\ -t_1t_4r_3e^{-\imath\Phi_4} & t_4r_1r_3e^{-\imath\Phi_4} & (r_4r_5-t_3t_4t_5)e^{-\imath\Phi_4} & -(t_5r_4+t_3t_4r_5)e^{-\imath\Phi_4} \\ -(t_2r_1+t_1t_3r_2)e^{-\imath\Phi_3} & -(t_1t_2-t_3r_1r_2)e^{-\imath\Phi_3} & t_5r_2r_3e^{-\imath\Phi_3} & r_2r_3r_5e^{-\imath\Phi_3} \end{pmatrix} \begin{pmatrix} \Psi_1 \\ \Psi_2 \\ \Psi_3 \\ \Psi_4 \end{pmatrix} = e^{\imath\omega} \begin{pmatrix} \Psi_1 \\ \Psi_2 \\ \Psi_3 \\ \Psi_4 \end{pmatrix} \tag{5}$$

Therefore, for one RG unit and a given set of t's and $\Phi_{0,j}$'s we obtain 3 level spacings s'_m. In order to achieve a reliable statistics, an average over many RG units is required in order to reach a smooth LSD $P(s)$. Thus the situation is comparable with estimating the true RMT emsemble distribution functions from small, say, 2×2 matrices only.[2,63]

Together with the RG approach for $P(t)$ we can now compute also $P(s)$ iteratively. We start with two chosen initial distributions (i) $P_0(t)$ which defines the transmittance of the SP's and (ii) $P_0(s)$ which enters in the energy dependence of phases Φ_j. The distributions $P_1(t)$ and $P_1(s)$ of the super-SP are then computed by averaging over results from many RG units. These new distributions are used iteratively for the next RG step and so on.

III. NUMERICAL RESULTS

A. The LSD at the QH transition

First, we are interested in the shape of the LSD at the QH transition. We choose the LSD of GUE as the starting distribution $P_0(s)$ of the RG iteration, since it is expected to be close to the critical LSD.[14] According to $P_0(s)$, we pick s_j and set Φ_j, $j=1,\ldots,4$ as in Eq. (4). For the transmission coefficients of the SP we use the FP distribution $P_c(t)$, obtained recently[23], as initial distribution $P_0(t)$. From $P_0(t)$, we choose t_i, $i=1,\ldots,5$. Using the RG transformation (1) we compute 10^7 super-transmission coefficients t'. The accumulated distribution $P_1(t')$ is discretized in at least 1000 bins, such that the bin width is typically 0.001 for the interval $t\in[0,1]$. $P_1(t')$ is then smoothed by a Savitzky-Golay filter[61] in order to decrease statistical fluctuations. From the solutions $\omega_j(E_k)=0$ of Eq. (3) the new LSD $P_1(s')$ is constructed using the "unfolded" energy level spacings $s'_m=(E_{m+1}-E_m)/\Delta$, where $m=1,2,3$, $E_{k+1}>E_k$ and the mean spacing $\Delta=(E_4-E_1)/3$. Due to the "unfolding"[64] with Δ, the average spacing is set to one for each sample and in each RG-iteration step we can superimpose spacing data of 2×10^6 super-SP's. The resulting LSD is discretized in bins with largest width 0.01. In the following iteration step we repeat the procedure using the P_1's as initial distributions. We assume that the iteration process has converged when the mean-square deviations of both distributions $P_n(t)$ and $P_n(s)$ deviate by less than

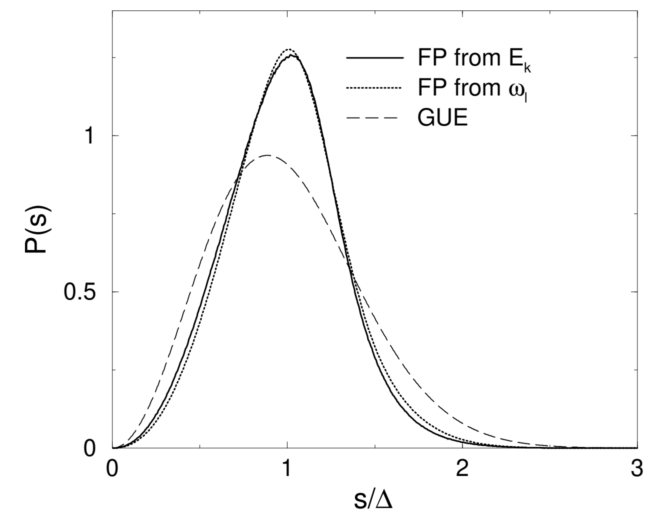

FIG. 3: FP distributions $P_c(s)$ obtained from the spectrum of $\omega_l(E=0)$ and from the RG approach using the real eigenenergies E_k in comparison to the LSD for GUE. As in all other graphs $P(s)$ is shown in units of the mean level spacing Δ.

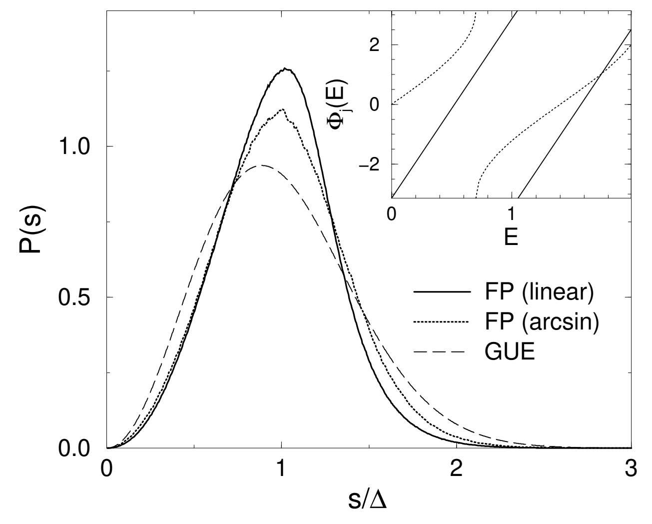

FIG. 4: FP distributions $P_c(s)$ for a linear and an arcsin energy dependence of the phases Φ_j. The form of $P_c(s)$ is clearly influenced by the actual choice of $\Phi_j(E)$. Thus we don't expect universal behavior in the bulk shape. The inset illustrates examples of the two different functions $\Phi_j(E)$ as in Eqs. (4) and (6).

10^{-4} from predecessors $P_{n-1}(t)$ and $P_{n-1}(s)$. Once the (unstable) FP has been reached, the P_n's should in principle remain unchanged during all further RG iterations. Unfortunately, our simulations show[23] that unavoidable numerical inaccuracies sum up within several further iterations and lead to a drift away from the FP. In order to stabilize our calculation, we therefore use in every RG step instead of $P_n(t)$ the FP distribution $P_c(t)$ obtained previously[23]. This trick does not alter the results and also speeds up the convergence of the RG for $P_c(s)$ considerably. The above approach now enables us to determine the critical LSD $P_c(s)$. The RG iteration converges rather quickly after only $2-3$ RG steps. The resulting $P_c(s)$ is shown in Fig. 3. Its shape is characterized by level repulsion for small s, a large maximum close to the mean level spacing Δ and a long tail.

Let us now also compare our results for the LSD with the FP distribution derived from the quasispectrum of phases ω_l. Since the ω_l's are obtained for fixed energy $E=0$, there is no energy dependence in the phase Φ_j of the RG unit in contradistinction to Eq. (4). Thus the Φ_j's contain only the random part and are uniformly distributed within $[0,2\pi]$. In Fig. 3 we show that both curves are almost identical. This observation is surprising, because the shape of $P_c(s)$ depends on the actual energy dependence of the phases Φ_j as in Eq. (4). Using instead of a linear E-dependence as in (4) another arbitrary functional form, say,

$$\Phi_j(E) = \Phi_{0,j} + 2\arcsin\left(\frac{E}{s_j} - 2p\right), \qquad (6)$$

where the periodicity is achieved by choosing the integer p such that $\left|\frac{E}{s_j} - 2p\right| \leq 1$, we find that the resulting $P_c(s)$ is indeed different from $P_c(s)$ as shown in Fig. 4. Therefore we can conlude that (i) the functional form of (4) is indeed a good guess and the assumption of Ref.[30] for the equivalence of ω_l and E_k approaches to computing the LSD is valid, (ii) the shape of $P_c(s)$ obtained from the E_k approach is non-universal and depends on the specific form of (4). We emphasize that a search for an *universal* form of $P_c(s)$ is flawed anyhow, as it has been shown recently that the critical LSD at a transition — although being system size independent — nevertheless depends on the geometry of the samples[65] and on the specific choice of boundary conditions.[66,67] It comes of course as no surprise that for our small RG unit, the influence of boundary conditions exerts a paramount influence.

B. Small and large s behavior

We now focus on two further characteristic properties of $P_c(s)$, the small s and the large s behavior, which have received considerable attention previously.[3–6,10,13,14,17,19,68] The shape of the LSD at the QH transition is a consequence of localization behavior of the wavefunction. For localized states a Poisson distribution is expected. In the delocalized regime the spatial extension of the wavefunction leads to an overlap and therefore to correlation between states and corresponding energy levels. Level repulsion is observed. For this case the LSD has been predicted by RMT[1], which was developed already in the 1950's to explain correlation in experimental nuclear spectra. This so called Wigner surmise, derived analytically for 2×2 matrices, relies on the symmetry of the underlying Hamiltonian. As already mentioned the contribution of the magnetic field breaks

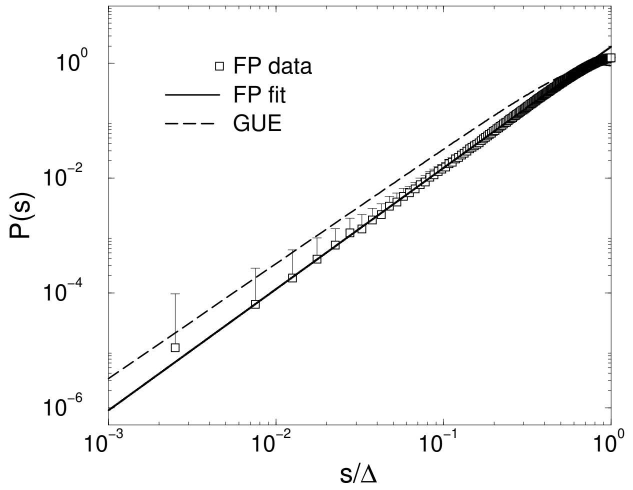

FIG. 5: FP $P_c(s)$ for small s in agreement with the predicted s^2 behavior. Due to the log-log plot errors are shown in the upper direction only.

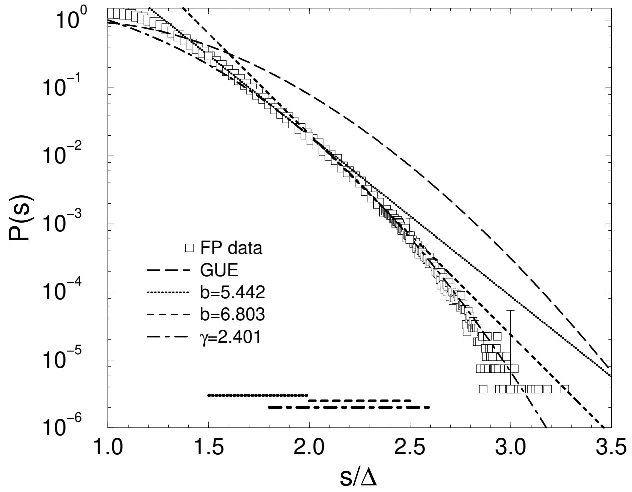

FIG. 6: The large s tail of the FP $P_c(s)$ compared with fits according to the predictions of Ref. 10 (dotted and dashed line) and 17 (dot-dashed line). The interval used for fitting is indicated by the bars close to the lower axis. For clarity error are shown in upper direction and for $s/\Delta = 1.5, 2.0, 2.5, 3.0$ only. For $s < 2.4$, only every 5th data point is shown by a symbol.

the time reversal symmetry. Therefore our case can be classified as belonging to the GUE for which

$$P_{GUE}(s) = \frac{32}{\pi^2} s^2 e^{-\frac{4}{\pi}s^2}. \tag{7}$$

The critical LSD at the transition lies between $P_{GUE}(s)$ and the Poisson distribution and inherits properties of both distributions.

For small s the critical LSD $P_c(s)$ is expected to behave like $P_{GUE}(s)$. It is governed by the s^2 dependence, indicating a strong level repulsion[3–5]. This holds also for our result, as can be seen in Fig. 5. The given error bars of our numerical data are standard deviations computed from a statistical average of 100 FP distributions each obtained for different random sets of t_i's and Φ_j's within the RG unit.

On the other hand the behavior of the large s tail of $P_c(s)$ has been discussed extensively[4,6,10,13,14,17,19,68]. The authors of Ref. 10 derived $P(s) \propto \exp(-as^\gamma)$ for $s \gg 1$ with $\gamma = 1 + (\nu d)^{-1}$. In our case we would therefore expect $\gamma \approx 1 + (2.35 \cdot 2)^{-1} \approx 1.23$. In early numerical simulations[6,19] for the 3D Anderson model of localization[18] general agreement with these relations was found. While in Ref. 19, γ coincided with the expected value, such quantitative agreement was not found in Refs. 6 and 13. Another kind of behavior was proposed in Ref. 17 where for the large s tail $P(s) \propto \exp(-bs)$ has been predicted with b as a system dependent constant related to the multifractality of the wavefunctions at criticality. This relation was numerically checked, e.g., in Refs. 4,14 and the discrepancy with earlier works was attributed to a higher numerical accuracy attainable with modern computers. For the QH transition $b \approx 4.1$ has been obtained[68] using the 2D Anderson model of localization with magnetic field.

In Fig. 6 we show our data with fits according to both behaviors. Our $P_c(s)$ decays rather fast. An exponential behavior can describe the large s tail only in limited intervals. We obtain $b = 5.442$ for $s/\Delta \in [1.5, 2.0]$ and $b = 6.803$ for $s/\Delta \in [2.0, 2.5]$ as decay coefficient compared to $b \approx 4.1$ of Ref. 68. The fit of Ref. 10 within the interval $[1.8, 2.6]$ yields better agreement with our data. However we find $\gamma = 2.401$ which also contradicts the expected value 1.23. We attribute these deviations to the low accuracy of the distribution in the required interval, which finally does not allow us to favor one or the other dependency.

At this point it seems that only the s^2 behavior of $P_c(s)$ for small s proves to be robust within our RG approach and obeys the expected universal level repulsion. But as we will show in the next section universality can be found also in additional quantities derived from the critical LSD.

IV. SCALING RESULTS FOR THE LSD

A. Finite-size scaling at the QH transition

As has been established experimentally, the QH transition is a 2nd order phase transition[69]. This kind of transition can be characterized by the divergence of a correlation length ξ_∞, e.g. the localization length of the wavefunction, according to

$$\xi_\infty(z_0) \propto |z_0 - z_c|^{-\nu} \tag{8}$$

when the controlling parameter z_0 reaches the critical point z_c. The value of critical exponent ν is usually[70,71] predicted to be a universal quantity.[72–74] For the QH transition ν has been calculated by a variety of numerical methods, e.g. $\nu = 2.5 \pm 0.5$[20], 2.4 ± 0.2[21], 2.35 ± 0.03[22], and 2.39 ± 0.01[23], which agrees also with the experimental estimates $\nu \approx 2.3$[69,75,76].

In order to extract ν from the LSD we employ the one-parameter-scaling hypothesis[77]. This theory describes the rescaling of a quantity $\alpha(N;\{z_i\})$ — depending on (external) system parameters $\{z_i\}$ and the system size N — onto a single curve by using a scaling function f

$$\alpha\left(N;\{z_i\}\right) = f\left(\frac{N}{\xi_\infty(\{z_i\})}\right). \tag{9}$$

Since Eq. (8), as indicated by "∞", holds only in the limit of infinite system size, we now use the scaling assumption to extrapolate f to $N \to \infty$ from the finite-size results of the computations. The knowledge about f and ξ_∞ then allows to derive the value of ν.

In our present study, we will use only the parameter z_0, which is connected to the RG of the LSD in the following way. Let us consider z as the dimensionless height of a SP in the potential according to the transformation rule $t = (e^z+1)^{-1/2}$.[52] Thus the distribution $P(G)$ can be translated easily to the distribution $Q(z)$ of the SP heights via $Q(z) = P(G)dG/dz = P\left[(e^z+1)^{-1}\right]/4\cosh^2(z/2)$. In Ref. 23, we have shown that that Q_c corresponding to P_c is a distribution function symmetric around $z = 0$ and close to a sum of Gaussians in is functional form. We then introduced the parameter z_0 as a shift in the initial distribution $Q_0(z) = Q_c(z - z_0)$.[23] For $z_0 < 0$ this disturbance in $Q_0(z)$ acts toward the localized regime since the weight in the corresponding $P(G)$ is moved toward conductance $G = 0$. The opposite holds for $z_0 > 0$. Here $Q_0(z)$ is shifted toward the delocalized regime ($G = 1$). Consequently, from the choice of the starting distribution of the RG iteration follows the position of transition at the critical value $z_c = 0$.

B. Scaling for α_P and α_I

In principle, we are now free to choose for the finite-size analysis any characteristic quantity $\alpha(N; z_0)$ constructed from the LSD which has a systematic dependence on system size N for $z_0 \neq 0$ while being constant at the transition $z_0 = 0$. Because of the large number of possible choices[7,14,17,68,78,79] we restrict ourselves to two quantities which are obtained by integration of the LSD and have already been successfully used in Refs. 7,80, namely

$$\alpha_P = \int_0^{s_0} P(s)ds \tag{10}$$

and second

$$\alpha_I = \frac{1}{s_0}\int_0^{s_0} I(s)ds, \tag{11}$$

with $I(s) = \int_0^s P(s')ds'$. The integration limit is chosen as $s_0 = 1.4$ which approximates the common crossing

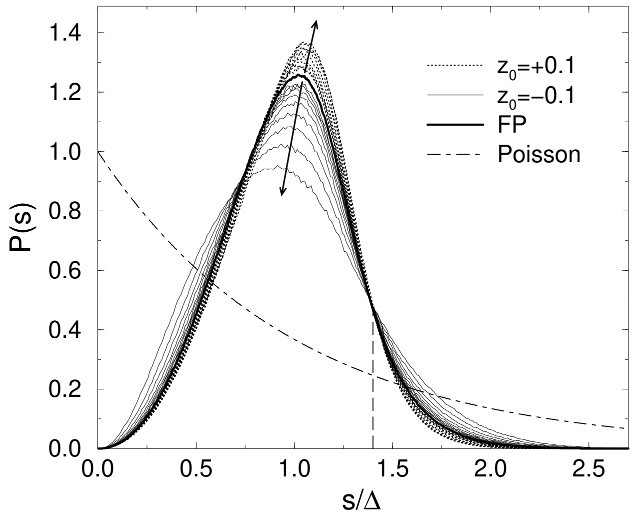

FIG. 7: RG of the LSD used for the computation of ν. The dotted lines corresponds to the first 9 RG iterations with an initial distribution P_0 shifted to the metallic regime ($z_0 = 0.1$) while the long-dashed lines represent results for a shift toward localization ($z_0 = -0.1$). Within the RG procedure the LSD moves away from the FP as indicated by the arrows. At $s/\Delta \approx 1.4$ the curves cross at the same point – a feature we exploit when deriving a scaling quantity from the LSD.

point[7] of all LSD curves as can be seen in Fig. 7. Thus $P(s_0)$ is independent of the distance $|z - z_c|$ to the critical point and the system size N. We note that N is directly related to the RG step n by $N = 2^n$. The double integration in α_I is numerically advantageous since fluctuations in $P(s)$ are smoothed. We now apply the finite-size-scaling approach from Eq. (9)

$$\alpha_{I,P}(N, z_0) = f\left(\frac{N}{\xi_\infty(z_0)}\right). \tag{12}$$

Since $\alpha_{I,P}(N, z_0)$ is analytical for finite N, one can expand the scaling function f at the critical point. The first order approximation yields

$$\alpha(N, z_0) \sim \alpha(N, z_c) + a|z_0 - z_c|N^{1/\nu} \tag{13}$$

where a is a coefficient. For our calculation we use a higher order expansion proposed by Slevin and Ohtsuki.[81] In their method f is expanded twice, first, in Chebyshev polynomials of order $\mathcal{O}_\nu$ and, second, as Taylor expansion with terms $|z_0 - z_c|$ in the order $\mathcal{O}_z$. This allows to describe deviations from linearity in $|z_0 - z_c|$ at the transition. Additionally they take into account also contributions from an irrelevant scaling variable with leads to a shift of the transition for small system sizes. As shown in Fig. 8, our data show the transition at $z_0 = 0$. Therefore we can neglect the influence of irrelevant variables. In order to obtain the functional form of f the fitting parameters, including ν, are evaluated by a non-linear least-square (χ^2) minimization. In Fig. 8 we show the resulting fit for α_P and α_I at the transition. The

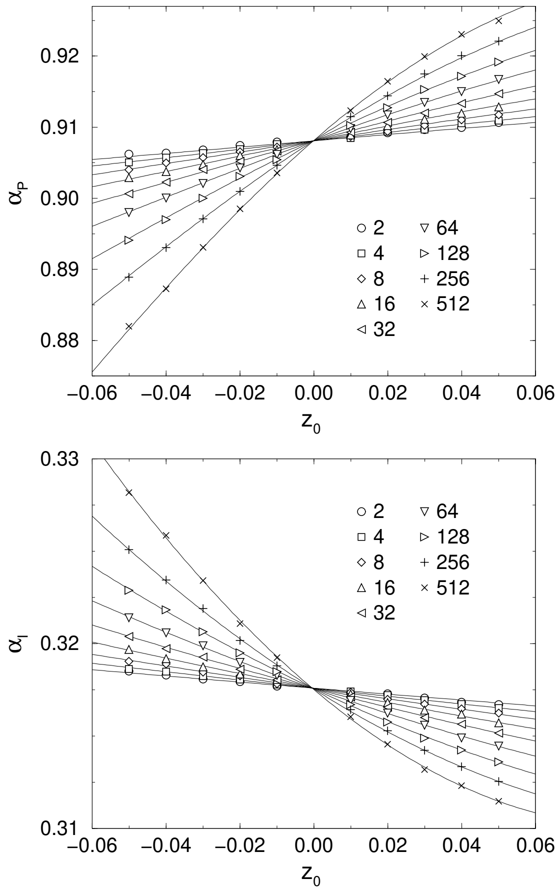

FIG. 8: Behavior of α_{I} and α_{P} at the QH transition as results of the RG of the LSD. Data are shown for RG iterations $n = 1, \ldots, 9$ corresponding to effective system sizes $N = 2^n = 2, \ldots, 512$. Full lines indicate the functional dependence according to FSS using the χ^2 minimization with $\mathcal{O}_\nu = 2$ and $\mathcal{O}_z = 3$.

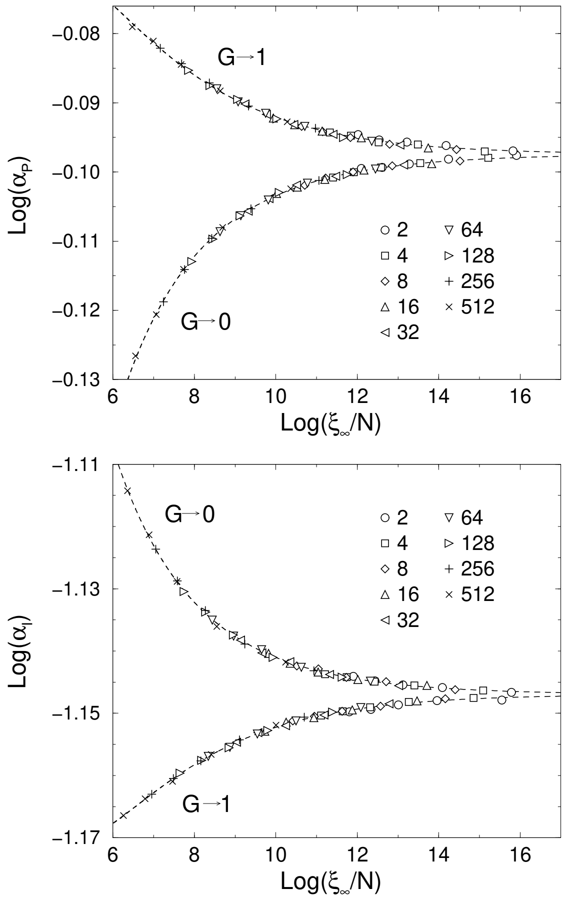

FIG. 9: FSS curves resulting from the χ^2 fit of our data shown in Fig. 8. Different symbols correspond to different effective system sizes $N = 2^n$. The data points collapse onto a single curve indicating the validity of the scaling approach.

fits are chosen in a way such that the total number of parameters is kept at a minimal value and the fit agrees well with the numerical data. The corresponding scaling curves are displayed in Fig. 9. In the plots the two branches for localized ($z_0 < 0$) and extended ($z_0 > 0$) regime can be distinguished clearly. In order to estimate the error of fitting procedure we compare the results for ν obtained by different orders $\mathcal{O}_\nu$ and $\mathcal{O}_z$ of the expansion, system sizes N, and regions around the transition. A part of our over 100 fit results together with the standard deviation of the fit are given in Table I. The value of ν is calculated as average of all individual fits where the resulting error of ν was smaller than 0.02. The error is then determined as the standard deviation of the contributing values. By this method we assure that our result is not influenced by local minima of the nonlinear fit. So we consider $\nu = 2.37 \pm 0.02$ as a reliable value for the exponent of the localization length at the QH transition obtained from the LSD. This is in excellent agreement with $\nu = 2.5 \pm 0.5$ (Ref. 20), 2.4 ± 0.2 (Ref. 21), 2.35 ± 0.03 (Ref. 22), and 2.39 ± 0.01 (Ref. 23) calculated previously.

We mention that besides α_{P} and α_{I} we tested also a parameter-free scaling quantity $\int_0^\infty s^2 P(s) ds$,[79] where the whole distribution $P(s)$ is taken into account. Here, due to the influence of the large s-tail only a less reliable value $\nu = 2.33 \pm 0.05$ was obtained.

C. Different initial distributions

Let us now study the influence of the initial conditions. So far we constructed the starting distributions $P_0(t)$ and $P_0(s)$ of the RG iteration by disturbing the critical distributions $P_{\mathrm{c}}(t)$ and $P_{\mathrm{c}}(s)$. Now we examine how $P_0(t)$ and $P_0(s)$ based on non-critical and therefore "wrongly chosen" distributions $P(t)$ and $P(s)$ would effect our results. E.g. we construct $P_0(t)$ from a distribution $P_{Gauß}(G)$ which is sharply peaked but still symmetric with respect to $G = 0.5$ as shown in Fig. 10. The corresponding LSD is obtained similar to the calculation of $P_{\mathrm{c}}(s)$, where we now use $P_n(G) = P_{\mathrm{Gauß}}(G)$ in all iterations.

For the determination of the critical exponent, we

TABLE I: Part of fit results for ν obtained from $\alpha_{\rm I}$ and $\alpha_{\rm P}$ for different system sizes N, intervals around the transition, orders $\mathcal{O}_\nu$ and $\mathcal{O}_z$ of the fitting procedure.

N	$[z_{0min}, z_{0max}]$	$\mathcal{O}_\nu$	$\mathcal{O}_z$	ν
		$\alpha_{\rm P}$		
$2-512$	$[9.93, 10.07]$	3	2	2.336 ± 0.010
$2-256$	$[9.93, 10.07]$	2	3	2.412 ± 0.013
$4-512$	$[9.95, 10.05]$	3	1	2.325 ± 0.014
$2-512$	$[9.95, 10.05]$	2	1	2.402 ± 0.014
$2-256$	$[9.95, 10.05]$	2	2	2.360 ± 0.016
$16-512$	$[9.95, 10.05]$	2	3	2.385 ± 0.018
$2-128$	$[9.93, 10.07]$	1	3	2.384 ± 0.019
$4-512$	$[9.93, 10.07]$	2	1	2.471 ± 0.019
		$\alpha_{\rm I}$		
$2-512$	$[9.93, 10.07]$	2	2	2.383 ± 0.010
$2-512$	$[9.93, 10.07]$	2	3	2.388 ± 0.010
$2-512$	$[9.93, 10.07]$	3	1	2.346 ± 0.012
$8-512$	$[9.93, 10.07]$	2	3	2.376 ± 0.012
$2-512$	$[9.95, 10.05]$	2	3	2.368 ± 0.014
$2-128$	$[9.93, 10.07]$	2	3	2.377 ± 0.016
$16-512$	$[9.95, 10.05]$	2	1	2.367 ± 0.016
$2-256$	$[9.93, 10.07]$	3	3	2.372 ± 0.018

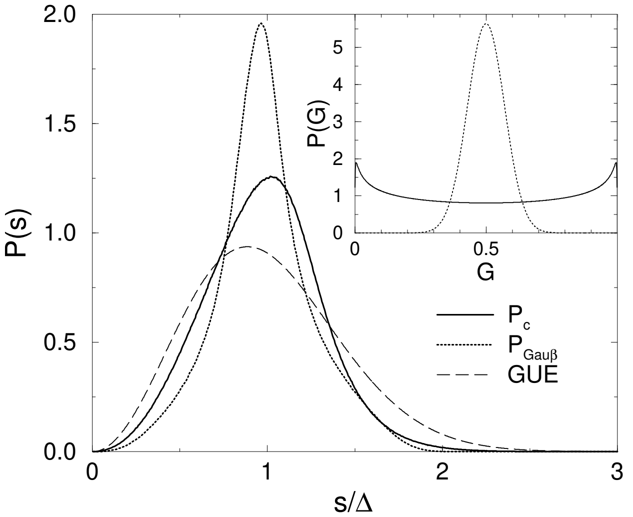

FIG. 10: Comparison of the LSD $P_{\rm c}(s)$ and $P_{Gau\beta}(s)$ obtained from the corresponding conductance distributions shown in the inset.

again disturb the distributions by an energy shift z_0 and study the change of the LSD in the course of the RG iterations by means of $\alpha_{\rm I}$ and $\alpha_{\rm P}$. Our data for $\alpha_{\rm I}$ are plotted in Fig. 11. The curves for small system sizes N exhibit strong deviations, i.e., there is initially no common crossing point, while for large N a behavior similar to Fig. 8 is observed. Therefore small N data are neglected in the scaling analysis. The χ^2 fits for $\alpha_{\rm I}$ and $\alpha_{\rm P}$ are carried out using $z_0 \in [-0.05, 0.05]$ and $N = 16-512$.

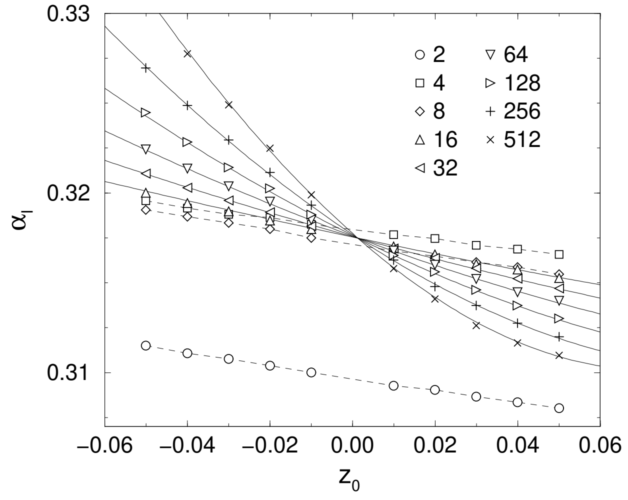

FIG. 11: Behavior of $\alpha_{\rm I}$ computed for initial distributions $P_{\rm Gauß}$ different from the critical distributions, as shown in Fig. 10. Data are plotted for RG iterations $n = 1, \ldots, 9$ corresponding to effective system sizes $N = 2^n = 2, \ldots, 512$. Curves for small n do not cross at the common point $z_0 = 0$. Full lines indicate the functional dependence according to FSS using the χ^2 minimization with $\mathcal{O}_\nu = 2$ and $\mathcal{O}_z = 2$.

They yield $\nu_{\rm I} = 2.43 \pm 0.02$ and $\nu_{\rm P} = 2.46 \pm 0.03$ which are still reasonable close to $\nu = 2.37 \pm 0.02$ obtained for the correct initial distributions. Obviously the initial failure is reduced and smeared out already after a few RG iterations. This is a fundamental property of this RG approach and strongly connected to the choice of the RG unit, which is constructed to capture the right chiral symmetry of the QH transition.

V. CONCLUSION

The common way to study the LSD in lattice or network models is to examine as large as possible systems. Only this allows to obtain a huge number of energy levels required for a reliable statistics and furthermore is a prerequisite to observe universal behavior. In this work we choose a different method. Instead of a large CC network we use only a 5 SP RG unit to extract the eigenenergies. This RG approach is based on an specific assumption of the energy dependence (4) of the phases in the RG unit, which has an influence also on the shape of the LSD. Therefore the overall form of the computed critical LSD $P_{\rm c}$ is not universal but at least shows a quadratic level repulsion for small s, one of the predicted characteristic properties. We checked that this behavior is observed also for a different nonlinear energy dependence of the phases in the RG unit.

The robustness of universal properties is moreover demonstrated by a finite-size scaling analysis of the LSD around the QH transition. The exponent $\nu = 2.37 \pm 0.02$ of the localization length obtained by a nonlinear χ^2 minimization is in excellent agreement with the value calculated in previous works.

This result is surprisingly good when keeping in mind that it was derived just from the 4 loops of our RG unit. Nevertheless this RG unit seems to capture the essential physics of the QH transition. We attribute the success of our RG approach to (i) the description of the transmission amplitudes t of the SP's by a correct distribution function $P(t)$, while for network models usually a fixed value $t(E)$ is assigned to all SP's, (ii) the phases are associated with full loops in the network and not with single SP-SP links, and (iii) a design of the RG unit describing the underlying symmetry of the QH transition, which is not accessible, e.g., with the 4 SP RG unit considered in Ref. 57. Due to these reasons the RG iteration is always governed by the quantum critical point of the QH transition. Even when starting the iteration with a distribution $P_0(G)$ totally different from $P_c(G)$, but still symmetric with respect to $G = 0.5$, we approach after a view iterations at the same results.

We argue that our findings indicate a large robustness of universal properties of the QH transition. Using a simple non interacting semiclassical picture of electron propagation and the rather crude RG approach we were able to reveal universal behavior. On the other hand experimental results[82,83] clearly indicate the influence of electron interaction at the QH transition. It seems that a fundamental description of QH transition is still far from being accomplished.

Acknowledgments

We thank R. Klesse and I. Zharekeshev for stimulating discussions. This work was supported by the NSF-DAAD collaborative research Grant No. INT-0003710. P.C. and R.A.R. also gratefully acknowledge the support of DFG within the Schwerpunktprogramm "Quanten-Hall-Systeme" and the SFB 393.

---

* Permanent address: Department of Physics, University of Warwick, Coventry CV4 7AL, UK, Email: r.roemer@warwick.ac.uk

1 E. P. Wigner, Ann. Math. **62**, 548 (1955).
2 M. L. Mehta, *Random Matrices and the Statistical Theory of Energy levels* (Academic Press, New York, 1991).
3 T. Kawarabayashi, T. Ohtsuki, K. Slevin, and Y. Ono, Phys. Rev. Lett. **77**, 3593 (1996), ArXiv: cond-mat/9609226.
4 M. Batsch, L. Schweitzer, I. K. Zharekeshev, and B. Kramer, Phys. Rev. Lett. **77**, 1552 (1996), ArXiv: cond-mat/9607070.
5 M. Metzler, J. Phys. Soc. Japan **67**, 4006 (1998).
6 S. N. Evangelou, Phys. Rev. B **49**, 16805 (1994).
7 E. Hofstetter and M. Schreiber, Phys. Rev. B **49**, 14726 (1994), ArXiv: cond-mat/9402093.
8 I. Varga, E. Hofstetter, M. Schreiber, and J. Pipek, Phys. Rev. B **52**, 7783 (1995), ArXiv: cond-mat/9407058.
9 M. Feingold, Y. Avishai, and R. Berkovits, Phys. Rev. B **52**, 8400 (1995), ArXiv: cond-mat/9503058.
10 V. E. Kravtsov, I. V. Lerner, B. L. Altshuler, and A. G. Aronov, Phys. Rev. Lett. **72**, 888 (1994).
11 L. Schweitzer and I. K. Zharekeshev, J. Phys.: Condens. Matter **7**, L377 (1995), ArXiv: cond-mat/9506072.
12 T. Ohtsuki and Y. Ono, J. Phys. Soc. Japan **64**, 4088 (1995), ArXiv: cond-mat/9509146.
13 S. N. Evangelou, Phys. Rev. Lett. **75**, 2550 (1995).
14 I. K. Zharekeshev and B. Kramer, Phys. Rev. Lett. **79**, 717 (1997), ArXiv: cond-mat/9706255.
15 M. Metzler and I. Varga, jpsj **67**, 1856 (1998).
16 M. Metzler, jpsj **68**, 144 (1999).
17 B. I. Shklovskii *et al.*, Phys. Rev. B **47**, 11487 (1993).
18 P. W. Anderson, Phys. Rev. **109**, 1492 (1958).
19 E. Hofstetter and M. Schreiber, Phys. Rev. Lett. **73**, 3137 (1994), ArXiv: cond-mat/9408040.
20 J. T. Chalker and P. D. Coddington, J. Phys.: Condens. Matter **21**, 2665 (1988).
21 D.-H. Lee, Z. Wang, and S. Kivelson, Phys. Rev. Lett. **70**, 4130 (1993).
22 B. Huckestein, Europhys. Lett. **20**, 451 (1992).
23 P. Cain, R. A. Römer, M. Schreiber, and M. E. Raikh, Phys. Rev. B **64**, 235326 (2001), ArXiv: cond-mat/0104045.
24 D. K. K. Lee and J. T. Chalker, Phys. Rev. Lett. **72**, 1510 (1994).
25 Z. Wang, D.-H. Lee, and X.-G. Wen, Phys. Rev. Lett. **72**, 2454 (1994).
26 D. K. K. Lee, J. T. Chalker, and D. Y. K. Ko, Phys. Rev. B **50**, 5272 (1994).
27 V. Kagalovsky, B. Horovitz, and Y. Avishai, Phys. Rev. B **52**, R17044 (1995).
28 V. Kagalovsky, B. Horovitz, and Y. Avishai, Phys. Rev. B **55**, 7761 (1997).
29 R. Klesse and M. Metzler, Europhys. Lett. **32**, 229 (1995).
30 R. Klesse and M. Metzler, Phys. Rev. Lett. **79**, 721 (1997).
31 I. Ruzin and S. Feng, Phys. Rev. Lett. **74**, 154 (1995).
32 M. Metzler, J. Phys. Soc. Japan **67**, 4006 (1998).
33 M. Janssen, M. Metzler, and M. R. Zirnbauer, Phys. Rev. B **59**, 15836 (1999).
34 R. Klesse and M. R. Zirnbauer, Phys. Rev. Lett. **86**, 2094 (2001), ArXiv: cond-mat/0010005.
35 B. Shapiro, Phys. Rev. Lett. **48**, 823 (1982).
36 P. Freche, M. Janssen, and R. Merkt, in *Proceedings of the Ninth International Conference on Recent progress in Many Body Theories*, edited by D. Neilson (World Scientific, Singapore, 1998), ArXiv: cond-mat/9710297.
37 R. Merkt, M. Janssen, and B. Huckestein, Phys. Rev. B **58**, 4394 (1998).
38 M. Janssen, Phys. Rep. **295**, 1 (1998), ArXiv: cond-mat/9703196.
39 P. Freche, M. Janssen, and R. Merkt, Phys. Rev. Lett. **82**, 149 (1999).
40 V. Kagalovsky, B. Horovitz, Y. Avishai, and J. T. Chalker, Phys. Rev. Lett. **82**, 3516 (1999).
41 J. T. Chalker *et al.*, (2000), ArXiv: cond-mat/0009463.
42 D.-H. Lee, Phys. Rev. B **50**, 10788 (1994).

[43] M. R. Zirnbauer, Ann. Phys. (Leipzig) **3**, 513 (1994).
[44] M. R. Zirnbauer, J. Math. Phys. **38**, 2007 (1997), ArXiv: cond-mat/9701024.
[45] I. A. Gruzberg, N. Read, and S. Sachdev, Phys. Rev. B **55**, 10593 (1997).
[46] A. W. W. Ludwig, M. P. A. Fisher, R. Shankar, and G. Grinstein, Phys. Rev. B **50**, 7526 (1994).
[47] Y. B. Kim, Phys. Rev. B **53**, 16420 (1996).
[48] C.-M. Ho and J. T. Chalker, Phys. Rev. B **54**, 8708 (1996), ArXiv: cond-mat/9605073.
[49] J. Kondev and J. B. Marston, Nucl. Phys. B **497**, 639 (1997), ArXiv: cond-mat/9612223.
[50] J. B. Marston and S. Tsai, Phys. Rev. Lett. **82**, 4906 (1999).
[51] D. P. Arovas, M. Janssen, and B. Shapiro, Phys. Rev. B **56**, 4751 (1997), ArXiv: cond-mat/9702146.
[52] A. G. Galstyan and M. E. Raikh, Phys. Rev. B **56**, 1422 (1997).
[53] A. Weymer and M. Janssen, Ann. Phys. (Leipzig) **7**, 159 (1998), ArXiv: cond-mat/9805063.
[54] M. Janssen, R. Merkt, and A. Weymer, Ann. Phys. (Leipzig) **7**, 353 (1998).
[55] M. Janssen, R. Merkt, J. Meyer, and A. Weymer, Physica **256–258**, 65 (1998).
[56] J. Sinova, V. Meden, and S. M. Girvin, Phys. Rev. B **62**, 2008 (2000), ArXiv: cond-mat/0002202.
[57] U. Zülicke and E. Shimshoni, Phys. Rev. B **63**, 241301 (2001), ArXiv: cond-mat/0101443.
[58] J. Bernasconi, Phys. Rev. B **18**, 2185 (1978).
[59] P. J. Reynolds, W. Klein, and H. E. Stanley, J. Phys. C **10**, L167 (1977).
[60] D. Stauffer and A. Aharony, *Introduction to Percolation Theory* (Taylor and Francis, London, 1992).
[61] W. H. Press, B. P. Flannery, S. A. Teukolsky, and W. T. Vetterling, *Numerical Recipes in FORTRAN*, 2nd ed. (Cambridge University Press, Cambridge, 1992).
[62] H. A. Fertig, Phys. Rev. B **38**, 996 (1988).
[63] E. P. Wigner, Proc. Camb. Phil. Soc. **47**, 790 (1951).
[64] F. Haake, *Quantum Signatures of Chaos*, 2nd ed. (Springer, Berlin, 1992).
[65] H. Potempa and L. Schweitzer, J. Phys.: Condens. Matter **10**, L431 (1998), ArXiv: cond-mat/9804312.
[66] D. Braun, G. Montambaux, and M. Pascaud, Phys. Rev. Lett. **81**, 1062 (1998), ArXiv: cond-mat/9712256.
[67] L. Schweitzer and H. Potempa, Physica A **266**, 486 (1998), ArXiv: cond-mat/9809248.
[68] M. Batsch and L. Schweitzer, in *High Magnetic Fields in Physics of Semiconductors II: Proceedings of the International Conference, Würzburg 1996*, edited by G. Landwehr and W. Ossau (World Scientific Publishers Co., Singapore, 1997), pp. 47–50, ArXiv: cond-mat/9608148.
[69] F. Hohls, U. Zeitler, and R. J. Haug, Phys. Rev. Lett. **88**, 036802 (2002), ArXiv: cond-mat/0107412.
[70] M. R. Zirnbauer, (1999), ArXiv: hep-th/9905054.
[71] M. Bhaseen *et al.*, Nucl. Phys. B **580**, 688 (2000), ArXiv: cond-mat/9912060.
[72] M. Janssen, O. Viehweger, U. Fastenrath, and J. Hajdu, *Introduction to the Theory of the Integer Quantum Hall effect* (VCH, Weinheim, 1994).
[73] B. Huckestein, Rev. Mod. Phys. **67**, 357 (1995).
[74] T. Chakraborty and P. Pietiläinen, *The Quantum Hall effects* (Springer, Berlin, 1995).
[75] S. Koch, R. J. Haug, K. v. Klitzing, and K. Ploog, Phys. Rev. B **43**, 6828 (1991).
[76] F. Hohls, U. Zeitler, and R. J. Haug, Phys. Rev. Lett. **86**, 5124 (2001), ArXiv: cond-mat/0011009.
[77] E. Abrahams, P. W. Anderson, D. C. Licciardello, and T. V. Ramakrishnan, Phys. Rev. Lett. **42**, 673 (1979).
[78] I. K. Zharekeshev and B. Kramer, Phys. Rev. B **51**, 17239 (1995).
[79] I. K. Zharekeshev and B. Kramer, Jpn. J. Appl. Phys. **34**, 4361 (1995), ArXiv: cond-mat/9506114.
[80] E. Hofstetter and M. Schreiber, Phys. Rev. B **48**, 16979 (1993).
[81] K. Slevin and T. Ohtsuki, Phys. Rev. Lett. **82**, 382 (1999), ArXiv: cond-mat/9812065.
[82] L. W. Engel, D. Shahar, C. Kurdak, and D. C. Tsui, Phys. Rev. Lett. **71**, 2638 (1993).
[83] W. Pan *et al.*, Phys. Rev. B **55**, 15431 (1997).